Formation of 3,3,4-Trimethyl-1,7-dibromonorbornane-2-one: a Spectroscopic and Computational Study

Ingrid T. Sabbagh and Perry T. Kaye*

Department of Chemistry, Rhodes University, Grahamstown, South Africa.

ABSTRACT

The structure and origin of the major by-product in the synthesis of 8-bromocamphor from (+)-3,3,8-tribromocamphor has been confirmed using NMR, coset and single crystal X-ray analysis and DFT-level computational techniques.

KEYWORDS

Camphor derivatives, skeletal rearrangement, DFT calculations, NMR, coset analysis.
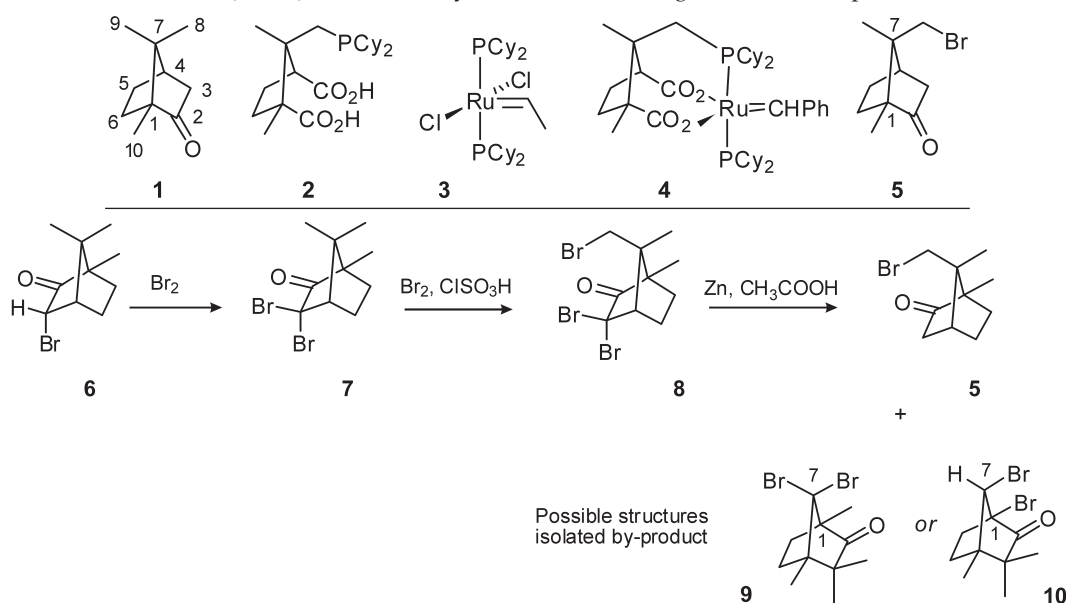
1. Introduction

In our research on the development of multidentate ligands for the construction of ruthenium complexes as novel metathesis catalysts,[1] we have targeted the D-(+)-camphor (**1**)-derived, tridentate ligand **2** in the expectation that coordination with ruthenium would afford the chelated analogue **4** of the first-generation Grubbs catalyst **3**.[2] Application of the method reported by Money and co-workers[3–6] afforded the critical precursor, 8-bromocamphor **5**, in 33 % overall yield from (+)-3-*endo*-bromocamphor **6**. In the final step [a Zn dust/AcOH-mediated reaction of (+)-3,3,8-tribromocamphor **8**] in the synthesis of this precursor, we isolated the desired product **5** in 44 % yield together with the major by-product, 3,3,4-trimethyl-1,7-dibromonorbornane-2-one **10**, in 10 % yield (Scheme 1). In this communication, we discuss the characterisation of 3,3,4-trimethyl-1,7-dibromonorbornane-2-one **10** and the use of DFT calculations to resolve conflicting mechanistic explanations for its formation.

One- and two-dimensional NMR spectroscopy of a by-product isolated during the synthesis of (+)-8-bromocamphor **5** appeared to be consistent with (1*R*,4*S*)-3,3,4-trimethyl-7,7-dibromonorbornan-2-one **9**. It was assumed that the by-product is formed during the reaction of the dibromo compound **7**, but the results of a coset[7] analysis of possible rearrangement pathways from 3,3-dibromocamphor **7** to compound **9** challenged this structural assignment.

In the coset analysis the maximum number of rearrangement steps in a given sequence was limited to 13 and the permissible operations to: Wagner-Meerwein rearrangements (WM), 2,3-*exo*- (23x), 2,3-*endo*- (23e) and 6,2- (62) shifts. Within these limits, the analysis generated the four potential pathways summarised in Fig. 1 for formation of compound **9** (in its protonated form **9H⁺**) from the protonated dibromocamphor starting material **7H⁺**; the rearrangement was expected to be acid-catalysed, thus warranting the use of protonated species.

The shortest sequence, the 7-step pathway (1) outlined in Scheme 2, commences with a Wagner-Meerwein rearrangement, followed by a 2,3-*endo*-methyl shift, a second Wagner-Meerwein and a 2,3-*endo*-bromide shift to afford intermediate **iv**. However, neither of the two subsequent steps, *viz.* the 2,3-*exo*-hydride shift to intermediate **v** nor the 2,3-*endo*-bromide shift to the *gem*-dibromide species **vi**, would be expected to be

Possible structures isolated by-product

Scheme 1

RESEARCH ARTICLE

I.T. Sabbagh and P.T. Kaye,
S. Afr. J. Chem., 2020, **73**, 30–34,
<https://journals.co.za/content/journal/chem/>.

31

1. WM 23e WM 23e 23x 23e WM
2. 23e 23x 23e 62 WM 62 WM 62
3. 23x 23e 23x 62 WM 62 WM 62
4. 62 WM 23e WM 23e WM 62 WM 62

WM = Wagner-Merwein
23e = 2,3-endo shift
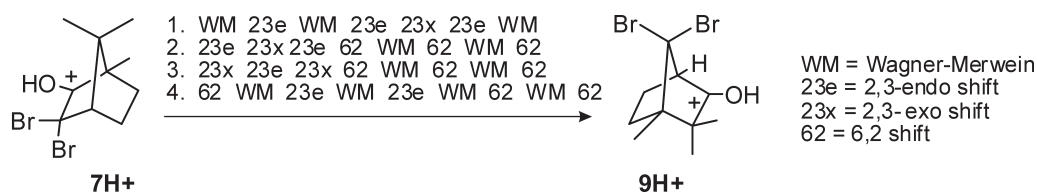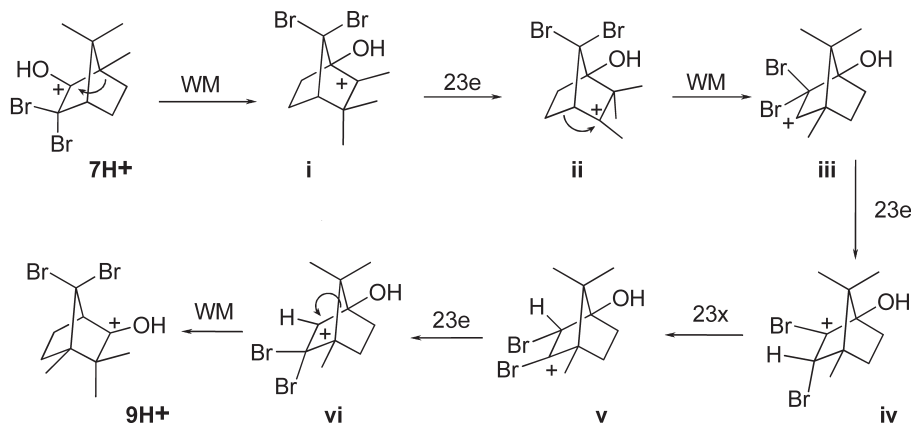23x = 2,3- exo shift
62 = 6,2 shift

Figure 1 Potential rearrangement pathways (**1–4**) for the formation of $9H^+$ from $7H^+$.

Scheme 2 Shortest coset sequence for the rearrangement of protonated structures $7H^+$ to $9H^+$.

energetically favoured. The 2,3-*exo*-hydride shift, while not impossible, is not likely to result in the relief of steric strain or the generation of a more highly substituted carbocation, while the 2,3-*endo*-bromide shift leads to the more sterically hindered species **vi**.

An examination of the alternative routes (2–4) to the cationic species $9H^+$ (Fig. 1) revealed the same energetically unfavourable hydride and bromide shifts in each pathway. These observations raised doubt concerning the assignment of structure **9**. Money and co-workers[3–6] had also isolated a by-product to which they assigned structure **10** using ^{1}H NMR data; this was subsequently supported by X-ray crystallographic analysis.[11] Re-examination of our one- and two-dimensional NMR data confirmed their consistency with structure **10**. Thus, the ^{1}H NMR spectrum clearly indicates the presence of: three methyl singlets at 1.08, 1.23 and 1.39 ppm; multiplets characteristic of the 5- and 6-methylene groups; and a singlet at 4.22 ppm corresponding to the relatively deshielded 7-methine proton. The ^{13}C NMR spectrum revealed the requisite number of methine, methylene, methyl, quaternary and carbonyl carbon signals, while the HMQC and HMBC data confirmed the proton-carbon connectivities – all of which, superficially at least, are also consistent with structure **9**! Single crystal X-ray analysis of the by-product isolated in our study[12] confirmed it to be the same as the compound isolated previously by Money and co-workers,[5] *viz.* 3,3,4-trimethyl-1,7-dibromonorbornan-2-one **10** and not the isomeric system **9**.

There remains, however, some disagreement about the mechanistic pathways followed in the transformation of 3,3-dibromo-camphor **7** to the by-product **10**. Money and co-workers had proposed[5] that 3,3,4-trimethyl-1,7-dibromonorbornan-2-one **10** was formed from the protonated intermediate $7H^+$ *via* the Wagner-Meerwein rearrangements, and the 2,3-*endo*-methyl and 2,3-*exo*-bromide shifts illustrated in **Pathway I** (Scheme 3). Antkowiak and Antkowiak,[13] on the other hand, argued that the Wagner-Meerwein shift from intermediate **12** to intermediate **13** was not feasible unless the carbon attached to the cationic centre bears *two* bromine atoms, as in structure **16**, reasoning that the steric effect of the dibromomethyl group renders the
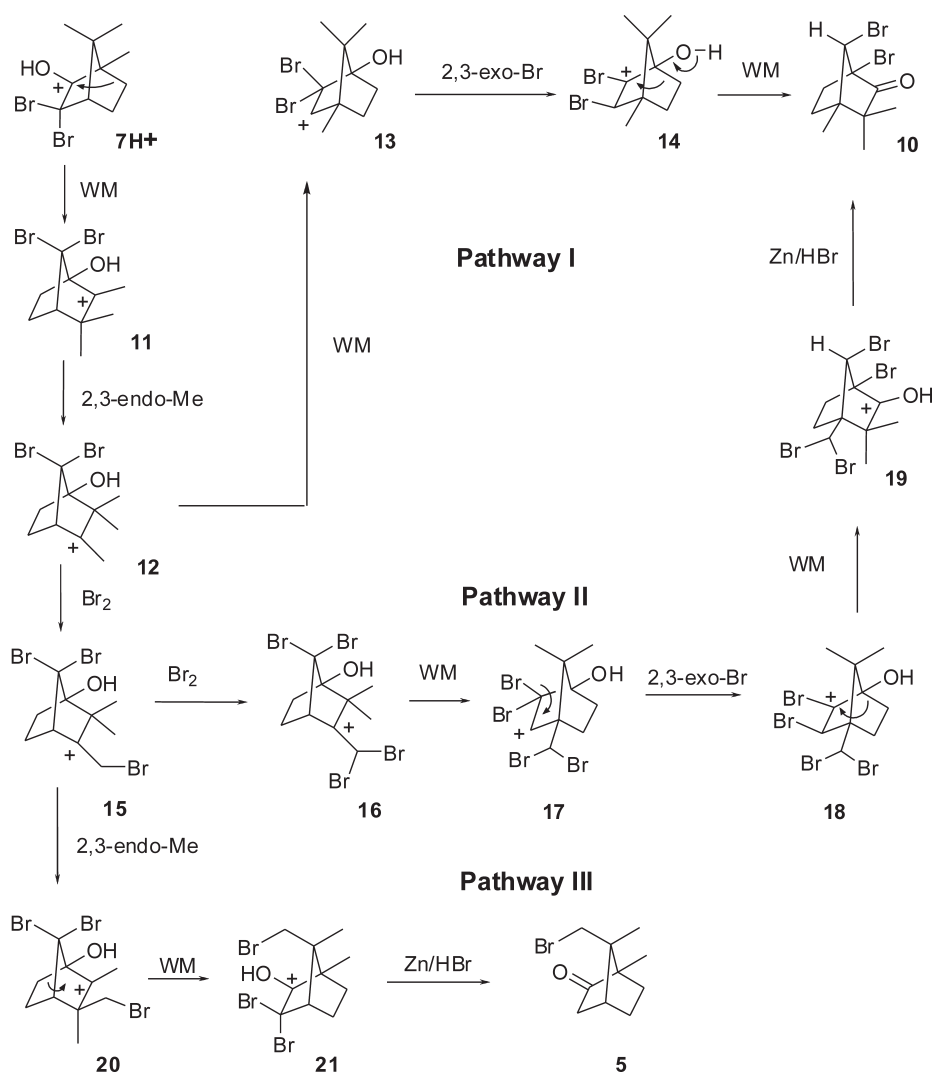
Wagner-Meerwein rearrangement **16 → 17** energetically preferable to the competing 2,3-methyl shift (as in the monobromomethyl case **15 → 20**). Consequently, they favoured **Pathway II**, in which compound **10** is formed as an intermediate during the final Zn dust/AcOH-mediated reaction of compound **19** which leads to 8-bromocamphor **5** and 3,3,4-trimethyl-1,7-dibromonorbornan-2-one **10**. **Pathway III** leads to the formation of 8-bromocamphor **5** from the intermediate **15**, as explored in our earlier paper.[2]

In order to explore the competing mechanistic proposals, we conducted a modelling study using the Accelrys DMol[3] DFT code in Materials Studio. Stable ground state structures could not be generated for either of the intermediates **13** or **14** in **Pathway I**. However, stable structures were located for the intermediates **16** and **18** in **Pathway II**. These species appear to be linked by a single transition state with a relatively low activation energy (7.59 kcal mol^{-1}), implying that the Wagner-Meerwein rearrangement (**16 → 17**) and the 2,3-*exo*-bromide shift (**17 → 18**) are, in fact, concerted. This transformation is detailed in Scheme 4, in which the transition state **TSI** approximates in structure to the tetrabromo intermediate **17**. An energetically favourable Wagner-Meerwein rearrangement of intermediate **18** then affords the tetrabrominated species **19** *via* a second transition state **TSII** (Scheme 5). The computational data for **Pathway II** are summarised in Table 1 and illustrated in Fig. 2.
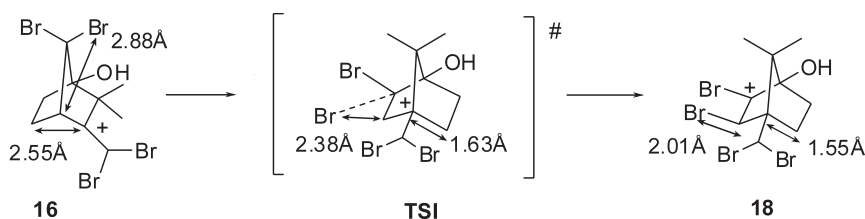
In our synthesis of 8-bromocamphor **5**, there was no spectroscopic evidence for the presence of the by-product **10** in the reaction mixture until after the final, Zn dust/AcOH-mediated reaction step. Both the computational and experimental evidence thus indicate **Pathway II**, as proposed by Antkowiak and Antkowiak,[13] to be a more likely route to compound **10** than

Table 1 DFT reaction energies (kcal mol^{-1}) for the rearrangements depicted in **Pathway II** (Scheme 3).

Reaction	ΔE	E_a	ΔG_{298}	$\Delta G^{\ddagger}_{298}$
16 → 18	–4.02	8.39	–5.06	7.59
18 → 19	–25.75	2.78	–24.75	2.45

RESEARCH ARTICLE

I.T. Sabbagh and P.T. Kaye,
S. Afr. J. Chem., 2020, **73**, 30–34,
<https://journals.co.za/content/journal/chem/>.

32

Scheme 3 Mechanistic pathways previously proposed for the transformation of 3,3-dibromocamphor **7** to the by-product **10**.
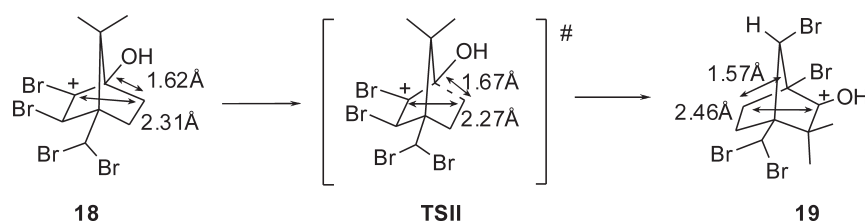

Scheme 4 Transformation **16 → 18**, showing significant inter-nuclear distances.

Pathway I, as suggested by Money and co-workers.[5] A combination of techniques, including coset, advanced one- and two-dimensional NMR and theoretical analysis, has thus permitted confirmation of the structure of a minor, terpenoid rearrangement product **10** and provided support for a mechanism involved in its formation.
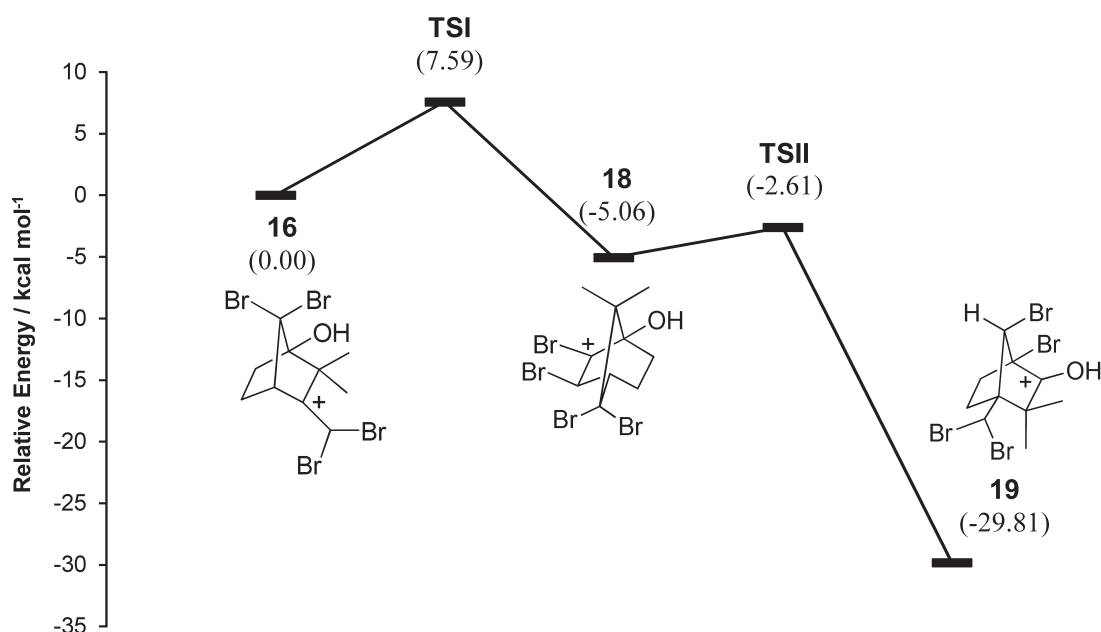
2. Experimental

2.1. General

NMR spectra were recorded on a Bruker AVANCE 400 MHz spectrometer at 303 K in $CDCl_3$, and calibrated using solvent signals. Infrared spectra were recorded on a Perkin Elmer FT-IR

Scheme 5 Transformation **18 → 19**, showing significant inter-nuclear distances.

Figure 2 Free energy diagram for **Pathway II** (**16 → 19**; Scheme 3). The gas-phase free-energies are presented in brackets.

Spectrum 2000 spectrometer. Low-resolution (EI) mass spectra were obtained on a Finnigan-Mat GCQ mass spectrometer. Optical rotations were measured on a Perkin Elmer 141 polarimeter using a 1 dm cell, with concentrations cited in g 100 mL^{-1}. Optically pure compounds were derived from commercially available, homochiral, (1R)-(+)-camphor.

(+)-8-Bromocamphor 5 and **(-)-3,3,4-Trimethyl-1,7-dibromo-norbornan-2-one 10** [3–5]

(+)-3,3,8-Tribromocamphor **8** (8.0 g, 20 mmol) was dissolved in glacial acetic acid (40 mL) in a round-bottomed flask. Zinc dust (4.4 g) was added, and the reaction mixture stirred vigorously while being cooled with ice-water. Stirring was continued for 1 h, during which time the exothermic reaction subsided. The solution was then decanted from the zinc salt into Et$_2$O (*ca.* 300 mL), and the resulting mixture was washed with water (10 × 50 mL) and dried over anhydrous MgSO$_4$. Removal of the solvent *in vacuo* afforded a brown oil (9.7 g) which was chromatographed [flash chromatography on silica gel; elution with hexane-EtOAc (9:1)] to afford two fractions.

i) (+)-8-Bromocamphor **5** (44 %)

An analytical sample was prepared by further chromatography [HPLC on Partisil 10; elution with hexane-EtOAc (9:1)], affording white crystals of (+)-8-bromocamphor **5**, m.p. 82–84 °C (lit.,[3] 83–85 ° C); $[\alpha]_D^{22}$ = +72.5 ° (*c* 0.80, CHCl$_3$), {lit.,[3] $[\alpha]_D^{25}$ = +76.7 ° (*c* 1.24, CHCl$_3$)}; δ_H (400 MHz; CDCl$_3$) 0.92 (3H, s, 9-CH$_3$), 1.14 (3H, s, 10-CH$_3$), 1.38 (1H, m, 5-H), 1.56 (1H, m, 6-H), 1.81 (1H, m, 6-H), 1.91 (1H, m, 5-H), 1.95 (1H, d, *J* 18.4 Hz, 3-H), 2.39 (1H, m, 3-H), 2.44 (1H, t, *J* 4.4Hz, 4-H), 3.10 (1H, d, *J* 11.0 Hz, 8-H) and 3.17 (1H, d, *J* 11.0 Hz, 8-H); δ_C (100 MHz; CDCl$_3$) 9.4 (C-10), 15.6 (C-9), 26.3 (C-5), 31.8 (C-6), 39.5 (C-8), 41.4 (C-4), 42.4 (C-3), 51.5 (C-1), 58.2 (C-7) and 217.8 (C-2); *m/z* 230/232 (M$^+$, 57 % / 55 %) and 107 (100).

ii) (1S,4S,7R)-3,3,4-Trimethyl-1,7-dibromonorbornan-2-one **10**

10 %, m.p. 117–119 C (lit.,[3] 123–124 °C); n$_{max}$(thin film)/cm^{-1} 1761 (C=O); $[\alpha]_D^{23}$ = –53.3 ° (c 1.05, CHCl$_3$) {lit.,[3] $[\alpha]_D^{23}$ = –51.5 ° (*c* 1.57, CHCl$_3$)}; δ_H (400 MHz; CDCl$_3$) 1.08 (3H, s, 9-CH$_3$), 1.23 (3H, s, 8-CH$_3$), 1.39 (3H, s, 10-CH$_3$), 1.68-1.74 (1H, m, 5-H), 2.09–2.12 (1H, m, 6-H), 2.12–2.15 (1H, m, 5-H), 2.29–2.32 (1H, m,

6-H) and 4.22 (1H, s, 7-H); δ_C (100 MHz; CDCl$_3$) 15.8 (C-8), 23.4 (C-10), 24.6 (C-9), 31.9 (C-5), 33.5 (C-6), 47.5 (C-4), 47.9 (C-3), 65.2 (C-7), 71.6 (C-1) and 210.7 (C-2); *m/z* 308 (M+, 4 %) and 159 (100).

2.2. Computational Methods

Density functional calculations were conducted using the Accelrys DMol^3 DFT code in Materials Studio (version 2.2)[14] on LINUX-based Pentium IV PCs. All calculations involved use of the generalized gradient approximation (GGA) functional by Perdew and Wang (PW91)[15] and the 'double numerical plus polarization' (DNP) basis set: a polarized split valence basis set of numeric atomic functions which are exact solutions to the Kohn-Sham equations for the atoms.[16] Geometry optimizations were subjected to convergence criteria of threshold values 2 × 10^{-5} Ha, 0.004 Ha/Å, 0.005 Å and 1 × 10^{-5} Ha for energy, force, displacement and self-consistent field (SCF) density, respectively. All calculations employed a method based on Pulay's[17] direct inversion of iterative subspace (DIIS) technique to accelerate SCF convergence using, where necessary, a small electron thermal smearing value of 0.005 Ha.

Preliminary transition state geometries were obtained using the integrated linear synchronous transit/quadratic synchronous transit (LST/QST) method,[18] and then subjected to full TS optimization using an eigenvector following algorithm. Where necessary, these geometries were confirmed using intrinsic reaction path (IRP) calculations, based on the nudged elastic band (NEB) algorithm,[19] to map the pathways connecting the relevant reactant, transition state and product geometries. All structures identified as stationary points were subjected to frequency analysis, to verify their classification as equilibrium geometries (zero imaginary frequencies) or transition states (one imaginary frequency). The reported energies reflect Gibbs free energy corrections to the total electronic energies at 298.15 K and include zero-point energy (ZPE) corrections.

RESEARCH ARTICLE

I.T. Sabbagh and P.T. Kaye,
S. Afr. J. Chem., 2020, **73**, 30–34,
<https://journals.co.za/content/journal/chem/>.

34

References

1 I.T. Sabbagh and P.T. Kaye, A computational study of Grubbs-type catalysts: structure and application in the degenerate metathesis of ethylene, *J. Molec. Struct.: THEOCHEM*, 2006, **763**, 37–42.

2 I.T. Sabbagh and P.T. Kaye, The regiospecific synthesis of 8-bromo-camphor revisited – A DFT computational study, *J. Molec. Struct: THEOCHEM*, 2007, **847**, 32–38.

3 C.R. Eck, R.W. Mills and T. Money, Synthetic route to 8-substituted camphor derivatives, *J. Chem Soc., Chem. Commun.*, 1973, 911–912.

4 C.R. Eck, R.W. Mills and T. Money, A new regiospecific synthesis of 8-bromocamphor, *J. Chem. Soc., Perkin Trans. 1*, 1975, 251–255.

5 P. Cachia, N. Darby, C.R. Eck and T. Money, Further observations on the bromination of camphor, *J. Chem. Soc., Perkin Trans. 1*, 1976, 359–362.

6 J.H. Hutchinson. T. Money and S.E. Piper, Ring cleavage of camphor derivatives: formation of chiral synthons for natural product synthesis, *Can. J. Chem.*, 1986, **64**, 854–860.

7 Based on a computational technique developed by Collins and Johnson[8,9] and refined in our group.[10]

8 C.J. Collins and C.K. Johnson, A computer-assisted analysis of the camphor-14c sulfuric acid reaction. Is 3,2-endo hydroxyl shift necessary? *J. Am. Chem. Soc.*, 1973, **95**, 4766–4768.

9 C.J. Collins and C.K. Johnson, Algebraic model for the rearrangements of 2-bicyclo[2.2.1]heptyl cations, *J. Am. Chem. Soc.*, 1974, **96**, 2514– 2513.

10 K.A. Lobb, unpubl. work.

11 C.A. Bear and J. Trotter, (-)-3,3,4-Trimethyl-1,7-dibromonorbornan-2-one, *Acta Cryst.*, 1975, **B31**, 904.

12 Sabbagh, I.S., *Metathesis Catalysts: an Integrated Computational, Mechanistic and Synthetic Study*, Ph.D. thesis, Rhodes University, 2005.

13 R. Antkowiak and W.Z. Antkowiak, Structure of some new minor products of 3-substituted camphor bromination. The stereospecificity of camphor methyl group functionalization, *Polish J. Chem.*, 1994, **68**, 2297.

14 B. Delley, An all-electron numerical method for solving the local density functional for polyatomic molecules, *J. Chem. Phys.*, 1990, **92**, 508–517; B. Delley, Fast calculation of electrostatics in crystals and large molecules, *J. Phys. Chem.*, 1996, **100**, 6107-6110. B. Delley, From molecules to solids with the DMol3 approach, *J. Chem. Phys.*, 2000, **113**, 7756–7764.

15 J.P. Perdew and Y. Wang, Accurate and simple analytic representation of the electron-gas correlation energy, *Phys. Rev. B.*, 1992,**45**, 13244–13249.

16 W. Kohn and L.J. Sham, Self-consistent equations including exchange and correlation effects, *Phys.* Rev., 1965, **140**, A1133.

17 P. Pulay, Improved SCF convergence acceleration, *J. Comp. Chem.*, 1982, **3**, 556–560.

18 T.A. Halgren and W.N. Lipscomb, The synchronous-transit method for determining reaction pathways and locating molecular transition states, *Chem. Phys. Lett.*, 1977, **49**, 225–232.

19 G. Henkelman and H. Jonsson, Improved tangent estimate in the nudged elastic band method for finding minimum energy paths and saddle points, *J. Chem. Phys.*, 2000, **113**, 9978–9985.